Chemical Geology xxx (2009) xxx–xxx

Contents lists available at ScienceDirect

Chemical Geology

journal homepage: www.elsevier.com/locate/chemgeo

Experimental approach of CO_2 biomineralization in deep saline aquifers

Sébastien Dupraz [a,b,*], Bénédicte Ménez [a,b], Philippe Gouze [c], Richard Leprovost [c], Pascale Bénézeth [d], Oleg S. Pokrovsky [d], François Guyot [a,b]

[a] Centre de Recherches sur le Stockage Géologique du CO_2 (IPGP/TOTAL/SCHLUMBERGER), case 89, 4 place Jussieu, 75252 Paris, cedex 05, France
[b] Equipe Géobiosphère Actuelle et Primitive, IPGP/IMPMC, case 89, 4 place Jussieu, 75252 Paris, cedex 05, France
[c] Géosciences Montpellier, CNRS UMR 5243, Université de Montpellier 2, place Eugène Bataillon, 34095 Montpellier, France
[d] Laboratoire des Mécanismes et Transferts en Géologie, UMR 5563– Université de Toulouse III – CNRS/IRD/OMP 14, avenue Edouard Belin, 31400 Toulouse, France

ARTICLE INFO

Article history:
Accepted 8 December 2008
Available online xxxx

Editor: J. Fein

Keywords:
CO_2 geological storage
Biomineralization
Carbonate precipitation
Bacillus pasteurii
Sporosarcina pasteurii
Ureolysis
Calcium bioassimilation
Geomicrobiology
Bacteria/mineral interactions

ABSTRACT

We describe an experimental system including monitoring of temperature, pressure, pH, oxidation reduction potential and optical density at 600 nm, designed for studying the role of microorganisms on the geological sequestration of CO_2 and its transformation into solid carbonate phases. Measurements were performed in an artificial ground water (AGW) supplemented with urea (2 $g.l^{-1}$) and equilibrated at controlled temperatures with a gaseous phase before bacterial inoculation. We used the ureolytic strain *Bacillus pasteurii* as a model carbonate precipitating bacteria and showed that it can successfully promote strong pH increases by ureolysis in the AGW equilibrated with CO_2 pressures of up to 1 bar. Increasing salinities (5.8, 13.5 and 35.0 $g.l^{-1}$) have a positive effect on the rate of pH increase, whereas the effect of increasing temperatures (30, 35 and 38 °C) is less important. Calcium is also shown to have a specific positive influence on the rate of ureolysis. The number of viable cells present in solution decreases greatly during the carbonate precipitation event but the population partially recovers once precipitation is over.

1. Introduction

Controlling CO_2 emission into the atmosphere has become one of the most important societal challenges since the recognition that global warming is most likely linked to human activity (IPCC, 2007). Nevertheless, the evolution toward a system free of fossil energies is slow and other methodologies limiting these emissions will have to be employed during the transition. Among them is the geological storage of CO_2 emitted by large industrial sources, where the produced gas would be injected, after purification and compression, into deep geological environments, namely oil and gas reservoirs as well as deep saline aquifers, deep-seated coal beds or (ultra)basic massifs (e.g. Haszeldine et al., 2005). Such environments are also now recognized to shelter extensive and active microbial communities that could possibly interact with the injected CO_2 (e.g. Pedersen, 2000; Amend and Teske, 2005), particularly in peripheral zones, far from the injection wells, where weaker CO_2 partial pressures allow microorganisms to overcome the toxicity of high levels of CO_2 (Wu et al., 2006). Despite the fact that our knowledge is poor regarding their biochemistry and the involved processes, it has already been established that these microorganisms are potentially able to induce CO_2 transformation into solid carbonates (e.g. Ménez et al., 2007). Hence, experimental work has been undertaken to tackle the importance of this process and the influence of the environmental parameters upon it. *Bacillus pasteurii* has been chosen as a reference microorganism for carbonate biomineralization regarding the fact that this microorganism and its metabolism, already employed in underground studies, have been extensively studied (e.g. Ferris et al., 2003; Mitchell and Ferris, 2005). This bacteria, now recognized as *Sporosarcina pasteurii* (Yoon et al., 2001), uses urea hydrolysis for both generating energy by ionic gradients (Mobley and Hausinger, 1989; Smith et al., 1993; Jahns, 1996) and as a source of nitrogen (Harder Nielsen et al., 1998; Swensen and Bakken, 1998). In parallel, urea hydrolysis leads to an increase in pH, which can induce carbonate precipitation by saturation with respect to calcite, aragonite and vaterite (Ferris et al., 1996; Stocks-Fischer et al., 1999; Dupraz et al., 2009—this issue).

During this biomineralization process, active transport of calcium appears to play a key role in *B. pasteurii* biochemistry, in addition to pH control. Exchangers and pumps are thought to generate calcium and proton gradients between the cell and the surrounding medium and to be responsible, to some extent, for the initiation of the precipitation in the cytoplasm or cell walls (McConnaughey and Whelan, 1997; Castanier et al., 1999; Hammes et al., 2003). Recently,

* Corresponding author. Current address: IPGP, Equipe Géobiosphère Actuelle et Primitive, case 89, 4 place Jussieu, 75252 Paris cedex 05, France. Tel.: +33 1 44 27 61 47; fax: +33 1 44 27 95 16.
E-mail address: dupraz@ipgp.jussieu.fr (S. Dupraz).

0009-2541/$ – see front matter © 2008 Elsevier B.V. All rights reserved.
doi:10.1016/j.chemgeo.2008.12.012

initial stages of calcification in *B. pasteurii* were demonstrated to be closely related to the precipitation of amorphous endocellular calcium phosphate (Dupraz et al., 2009—this issue). Nonetheless, the calcium content in solution was also proven, by the same authors, to directly influence the pH of the medium by formation of complexes. In the present study, to avoid effects induced by pH variations, experiments at fixed pH were first carried out with *B. pasteurii* in a pH stat to determine independently the specific influence of calcium. The effects of temperature and salinity were then investigated since they are key parameters for microbial proliferation in deep geological environments. The influence of CO_2 partial pressure increase was finally examined. For this purpose, a specific instrumentation called biomineralization control cell (BCC) was designed. It allows, in particular, to assess the intensity of the alkalinization and the biochemical conditions leading to the carbonate precipitation, by continuously recording temperature, pressure, pH, oxidation reduction potential (ORP) and optical density at 600 nm (OD_{600}), without causing any disruption in the studied processes. Experiments under higher CO_2 partial pressures were also performed in a specialized batch reactor.

2. Materials and methods

2.1. Artificial ground water

The artificial ground water (AGW) medium used during these experiments was prepared in ultra pure water (UPW, resistivity = 18 Ω) and based on the aqueous chemistry of the Dogger aquifer (Paris Basin, France), a limestone assemblage (200–300 m thick) of Middle Jurassic age, presenting a maximum burial depth of 1900 m below sea level. This stratigraphic level constitutes one of the possible pilot sites for CO_2 sequestration in France. The saline solutions from the aquifer are essentially of the NaCl type with relatively low Ca concentrations (i.e. around 20 mM). The average composition of the 67 °C Dogger level (Azaroual et al., 1997) was simulated in the AGW. This included $NaHCO_3$ (40 mM), $KHCO_3$ (2 mM), $MgSO_4,7H_2O$ (8 mM), $CaCl_2$ (20 mM) and NaOH (2 mM). The solution was complemented with urea (2 $g.l^{-1}$) and equilibrated with atmosphere at room temperature by acidification with hydrochloric acid (44 mM). The equilibrium was reached after an overnight of CO_2 degassing (coming from the dissolved inorganic carbonate species) and the pH of the unbuffered solution was then adjusted to 6.01. This refers to the standard AGW solution, displaying a final ionic strength of 0.135 M and a salinity (S) of 5.8 $g.l^{-1}$. For AGW without calcium, the formulation remains the same but with no addition of $CaCl_2$, leading to a final ionic strength of 0.076 M ($S = 3.6\ g.l^{-1}$). AGWs of different salinities were also realized by adding NaCl salt to the original composition. Once sterilized by Millipore filtration (0.2 μm Isopore™), the solutions were kept at 4 °C before the start of the experiments (t_0).

2.2. Bacterial growth and inoculation

B. pasteurii was grown in brain heart broth (MERCK) complemented with 20 $g.l^{-1}$ of urea. Mother solutions were freshly inoculated with the strain ATCC11859 (DSM 33) from DSMZ and kept overnight at 30 °C with agitation (200 rpm). Daughter cells that had succeeded to sustain an exponential growth were collected by centrifugation (8500 *g*, 10 min). The supernatant was then discarded and the resuspended pellet was rinsed with UPW. The procedure was repeated twice and pellets were used afterward as inoculation material for the experiments. For this purpose, cells were suspended in sterile UPW and then mixed at t_0 in equal parts with amended double strength AGW at a final OD_{600} of 0.05. All the solutions were thermally equilibrated to the experiment temperature before use.

2.3. Biomineralization control cell

The BCC (Fig. 1) is a closed circulating cell composed of four main parts: (a) the pump (diaphragm FEM 03 RC Stepdos™ pump coupled to a Teflon® Stepdos™ head) activating the fluid circulation at 20 $ml.min^{-1}$; (b) an equilibration tank (volume = 1 l) that allows the solution to equilibrate at a given pressure with a chosen gas composition, continuously regulated in the headspace. The headspace is associated to a tared valve (1 bar) and a gas entrance connected to a manometer. All the inner parts of the tank are made of Teflon® and both volume of the liquid and gas phases are equal to 500 ml. Mechanical stirring with bar magnet of the system was allowed in the equilibration tank, which represents more than 90% of the total volume of the circuit; (c) the

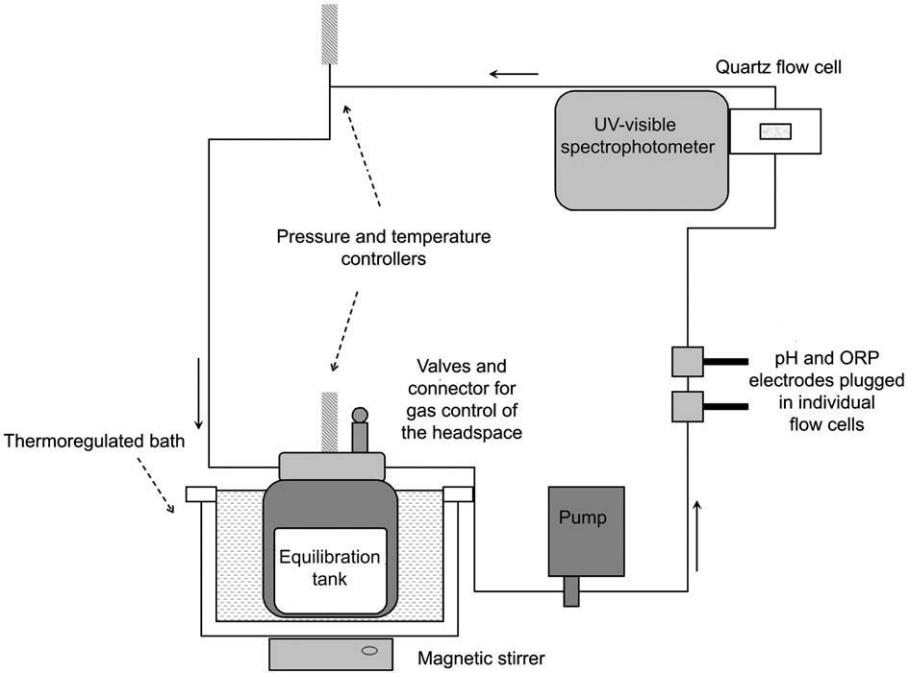

Fig. 1. Schematic description of the biomineralization control cell (BCC) apparatus. Circuit is closed and fluid submitted to an anti-clockwise motion by the pump.

Please cite this article as: Dupraz, S., et al., Experimental approach of CO_2 biomineralization in deep saline aquifers, Chem. Geol. (2009), doi:10.1016/j.chemgeo.2008.12.012

sensors that follow the evolution of the biomineralization process: a quartz flow cell coupled to a UV–visible Shimadzu spectrophotometer (UV-1650 PC), two temperature and pressure controllers directly connected to headspaces (Keller 35× coupled in parallel to a K107 Converter) plus Teflon® circulation cells containing separately two Fisherbrand double-junction gel-filled electrodes (pH and ORP); (d) the circuit that transfers the fluids all along the different parts and that is made of 1.6–3.2 mm (internal and external diameters, respectively) polypropylene tubes connected by Luer Lock® and Swagelok® vanes and connectors. Each device is connected to a computer that logs the data. Overall, the BCC is able to sustain a maximal differential pressure of 3 bar and temperatures up to 60 °C. The entire circuit was sterilized by a bleach treatment (6 $g.l^{-1}$ of active chlorine during 30 min) and then rinsed four times with 500 ml of sterilized UPW before injection of the AGW.

To test the impact of temperature and salinity on *B. pasteurii* metabolism and subsequent alkalinization, experimentations were run in BCC at different temperatures (30, 35 and 38 °C with S of 5.8 $g.l^{-1}$), and different salinities (5.8, 13.5 and 35 $g.l^{-1}$ at 30 °C). Finally, a third experiment was made with a symmetric combination of these two parameters (S = 13.5 $g.l^{-1}$ at 35 °C and S = 35 $g.l^{-1}$ at 38 °C). For all these runs, the headspace of the BCC equilibration tank was initially filled with atmospheric air at 1 bar without renewing, and agitation was applied to the solution. Other experiments were also run under standard conditions (S = 5.8 $g.l^{-1}$ at 30 °C with agitation) using an AGW without calcium or using a specific gas phase in the headspace, namely 1 bar of CO_2 or N_2. Note that owing to the high used flow rates, cells were mostly suspended in the device.

As the variations of calcium concentration in the bulk phase are either due to calcium carbonate precipitation, to adsorption on organic matter or to assimilation by cells (Dupraz et al., 2009—this issue), precipitation of calcium carbonate was, for all experiments, followed and quantified according to the observed discontinuities in pH and turbidity measurements.

2.4. pH stat

Experiments at constant regulated pH were conducted with a Schott titration instrument (Titroline alpha plus, TA10plus) that was programmed to stabilize the pH variation induced by *B. pasteurii* ureolysis to a fixed value of 8 by adding HCl solution of 0.1 M to the medium (reproducibility = 0.05%). Inoculated AGW solution was maintained in an open beaker at room temperature with mechanical stirring using bar magnets. Two experiments were accomplished with standard AGW and Ca-free AGW, respectively. Volumes of injected HCl solution, as well as pH, were continuously recorded while calcium concentration and OD_{600} were measured separately from aliquots. Soluble calcium content was determined with a flame atomic absorption spectrometer (Perkin Elmer 5100PC) with an uncertainty of 1%. Measurements of OD_{600} were performed on pre-acidified samples (addition of an equal volume of HCl 1 M) with a UV–visible dual beam spectrophotometer Varian Scan-50. All measurements were corrected from dilution effect induced by the addition of HCl solution. Nevertheless, the relatively low volume increase (i.e. 36 ml and <45 ml for the initial and final volumes,

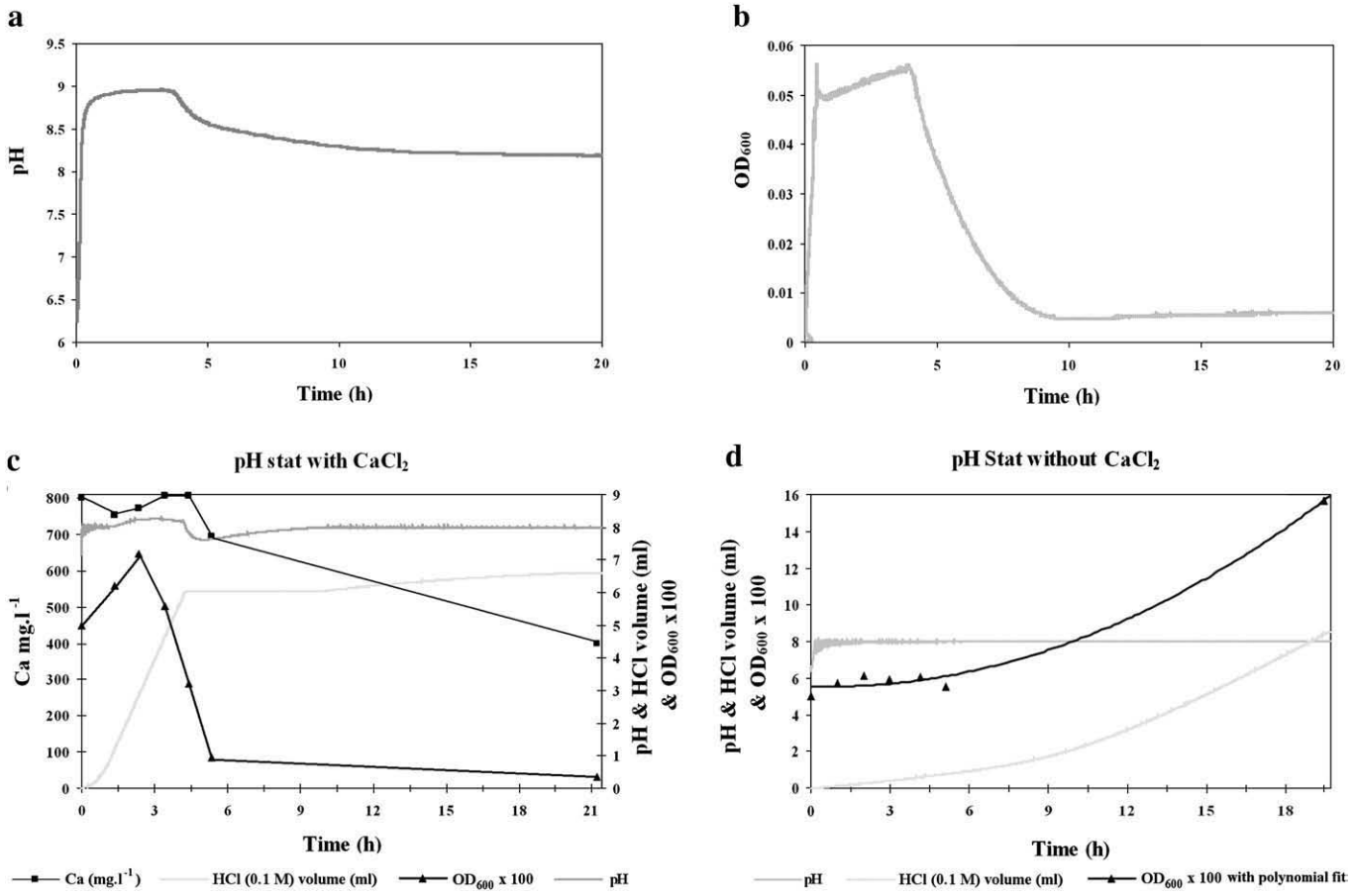

Fig. 2. pH (a) and OD_{600} (b) as a function of time for a BCC experiment run in artificial ground water (AGW) of salinity equal to 5.8 $g.l^{-1}$ at 30 °C and in contact with closed air atmosphere. pH stat experiments performed in AGW under a regulated pH value of 8 at ambient temperature with (c) and without $CaCl_2$ (d) with respective salinities of 5.8 and 3.6 $g.l^{-1}$. Both of these experiments were run in beakers opened to the atmosphere.

Please cite this article as: Dupraz, S., et al., Experimental approach of CO_2 biomineralization in deep saline aquifers, Chem. Geol. (2009), doi:10.1016/j.chemgeo.2008.12.012

respectively) ensured that no strong variations occurred in the system global chemistry.

2.5. Batch reactor for elevated pressure experiments

For experiments that needed pressures higher than 3 bar, a batch reactor, with controlled headspace pressure, was employed. It consists in a 450 ml closed-system high-pressure Ti batch reactor, containing the reactive solution, continuously stirred with a Parr magnetically driven stirrer. Carbon dioxide was delivered in the reactor through a Ti porous filter and CO_2 partial pressure was controlled by calibrated pressure manometer. Solution samples were taken using a valve equipped with a back-pressure regulator. Solution pH was measured *in situ* by means of a solid contact Li–Sn alloy commercial pH electrode (Potential®, St. Petersburg, Russia) coupled with a home-made Ag/AgCl reference electrode (see details in Pokrovsky et al., 2005).

2.6. Tests of viability

To assess the potential of optical density as reliable indicator of cell viability and thus evaluate if a linear correlation exists between the OD_{600} and the survival of bacteria, specific runs of alkalinization and calcium carbonate precipitation by *B. pasteurii* in AGW were launched in open Erlenmeyer flasks submitted to agitation (200 rpm) at 30 °C. Mac Grady tests were then undertaken on 40 ml of standard AGW solution inoculated with a final OD_{600} of 0.12, allowing more sensitive spectrophotometric measurements, compared to smaller inoculum size. For this purpose, aliquots of 1 ml were periodically sampled to measure pH together with OD_{600} and to determine the most probable number (MPN) of Mac Grady, following the procedure described in Hugues and Plantat (1983). Cultivability in brain heart broth (incubated 10 days at 30 °C) was tested in triplicates by diluting the sample in phosphate-buffered saline pH 7.2 solution (130 mM NaCl, 7 mM Na_2HPO_4, 30 mM NaH_2PO_4) using dilution factors of 10^6, 10^7 and 10^8.

2.7. Microscopic observations

Mineral phases were collected after centrifugation (8500 *g*, 10 min). The pellets were then quickly washed with Prolabo Rectapur™ ethanol and dried at 40 °C for 24 h. Microstructures and semi-quantitative chemical compositions were investigated by Scanning Electron Microscopy (SEM) with a ZEISS Supra 55VP, equipped with an Energy Dispersive X-ray Spectrometer (EDS). Images in secondary electron (SE) or in backscattered electron (BSE) modes were collected on metallized samples (carbon) at 2 or 7 kV and 3 nA and analysis were performed at 20 kV. Mineral identification benefited from powder X-ray diffraction (XRD) measurements performed in a previous study (Dupraz et al., 2009—this issue).

3. Results

3.1. Calcium

Changes in pH and OD_{600} of solutions, measured either in the BCC or in the pH-stat, and calcium evolution measured for the pH stat experiment after inoculation of *B. pasteurii* in AGW supplemented with urea under standard conditions (S = 5.8 g.l^{-1} at 30 °C with agitation) are summarized in Fig. 2 (Fig. 2a, b for BCC and Fig. 2c, d for pH stat, respectively). The characteristic pH and OD_{600} trends observed from BCC experiments (Fig. 2a and b) are similar to those from batch experiments, previously explained in detail and modelled in Dupraz et al. (2009-this issue): reaction begins with an increase in pH due to ureolysis that leads to a plateau, the value of which mostly depends on gas–liquid interfacial exchanges. Once a critical over-saturation with respect to solid calcium carbonates is reached, precipitation occurs and consumes carbonate ions, resulting in a pH decrease (e.g. Ferris et al., 1996; Stocks-Fischer et al., 1999). Critical over-saturation values necessary to precipitate calcium carbonates have been discussed in Ferris et al. (2003) and Dupraz et al. (2009-this issue). Precipitation of solid carbonates coincides with OD_{600} decrease (Fig. 2a and b). The pH-stat experiments exhibit the same phenomena, except that they are carried out at constant pH values by continuous addition of HCl. Considering that the system we used was designed for regulating pH increases, small pH deviations occurred in case where protons were released (e.g. precipitation in Fig. 2c). Moreover, the regulation was sometimes overwhelmed when the alkalinization process was too fast, as shown for example in the first part of the HCl volume curve in Fig. 2c. However, under conditions where pH remains stable, the added volume of HCl solution can be considered as a good indicator of the ureolytic production, which is larger in standard AGW than in calciumless experiments. When calcium is supplied to the reaction medium, the precipitation is strong, as reflected by the Ca concentration decrease and the slight fluctuation of the pH curve (Fig. 2c). This finally leads to decreased medium turbidity by sedimentation of the precipitates. As a result, when Ca-bearing AGW is used, OD_{600} decreases together with pH and Ca concentration (Fig. 2a, b and c). In contrast, pH-stat experiments conducted without calcium show a quasi constant OD_{600} (Fig. 2d), whereas a small quantity of precipitates can still be obtained (see discussion below). In this calciumless case, heavy centrifugation steps are required to collect the small amount of precipitates which are qualitatively different from those obtained in experiments with calcium and morphologically identified as vaterite and rhomboid calcite crystals by SEM observations. These precipitates exhibit high densities of cellular prints when compared to those collected from solutions containing calcium (Fig. 3).

3.2. Viability

The fall of OD_{600} associated to calcium carbonate precipitation suggests that precipitation is a highly lethal event for the bacterial population. Experiments were thus designed to compare OD_{600} and the MPN of the Mac Grady tests at this stage of the biomineralization process. Results are shown in Fig. 4. OD_{600} is representative of medium turbidity that could be either associated with bacterial, mineral or any other colloidal content of the bulk phase. On the other hand, Mac Grady test is accountable for the quantity of viable individuals (i.e. colony-forming units) that are able to initiate a bacterial growth. The pH evolution is similar to that of all the other experiments (see Fig. 2a for comparison). The OD_{600} and MPN values show an asymmetry

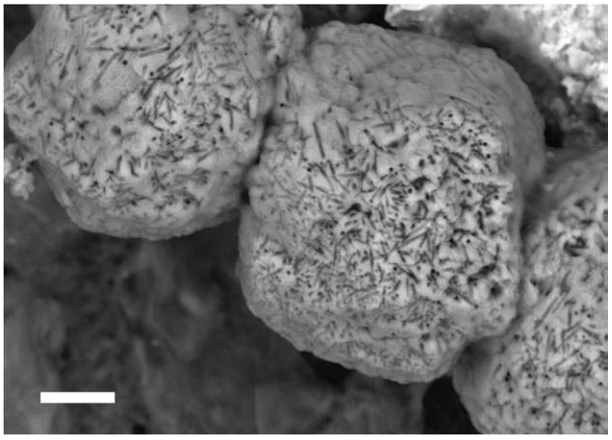

Fig. 3. Scanning electron microscopy (SEM) observation in backscattered electron mode (BSE) of precipitates yielded by pH stat experiment conducted in AGW without calcium (S = 3.6 g.l^{-1} at room temperature with agitation). Grains show a high density of cell prints that is not observed in other experiments to such extent (scale bar = 12 μm).

Please cite this article as: Dupraz, S., et al., Experimental approach of CO_2 biomineralization in deep saline aquifers, Chem. Geol. (2009), doi:10.1016/j.chemgeo.2008.12.012

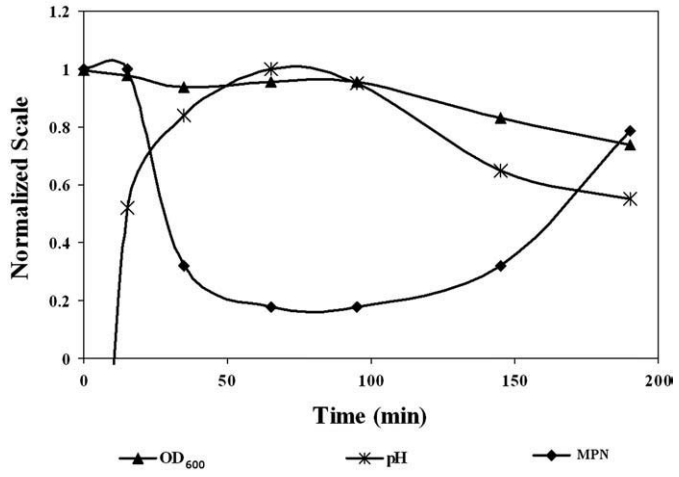

Fig. 4. Cellular mortality during precipitation in AGW (5.8 $g.l^{-1}$, 30 °C, open atmosphere) with a double inoculum size (OD_{600} = 0.12), compared to standard conditions. Data have been normalized to 1 to allow direct comparisons. Mac Grady MPN shows a strong asymmetry with the OD_{600} measurements and thus underlines the complex relationship existing between precipitation and cellular mortality.

between their trends. While the OD_{600} remains quite stable at the beginning and decreases in the second half of the experiment, the MPN values decrease very quickly in the first hour and then increase again after 2 h.

3.3. Salinity and temperature

BCC experiments were also carried out for investigating the role of temperature and salinity on the alkalinization process. Seven experiments were performed with combined values of 30, 35 and 38 °C temperatures and 5.8, 13.5, and 35.0 $g.l^{-1}$ salinities, respectively. Results are shown in Fig. 5. Four key variables are expressed as a function of temperature and salinity namely the maximum pH reached (Fig. 5a), the beginning of precipitation monitored from discontinuities either in OD_{600} (Fig. 5b) or in pH (Fig. 5c) and finally, proton release from $CaCO_3$ precipitation, resulting from the transformation of hydrogenocarbonate (HCO_3^-) into carbonate (CO_3^{2-}) ions (Fig. 5d). The pH trends of these tests follow the behavior described in Fig. 2a. The results displayed in Fig. 5a demonstrate a strong influence of salinity, which significantly increases the maximum pH reached, and thus the ureolysis rate. The temperature effects are rather small over the investigated range. The tests show a good correlation between the starting times of bulk precipitation as monitored by following either OD_{600} shift (Fig. 5b) or pH shift (Fig. 5c). It was systematically observed that OD_{600} decrease systematically occurred after the pH drop (i.e. a delayed estimated beginning of the precipitation when monitored by OD_{600}) with the exception of one test (30 °C, 35 $g.l^{-1}$) where the decrease in OD_{600} was observed 71 min before the pH decrease. Fig. 5d displays the quantity of protons released between the beginning and the end of the precipitation. Indeed, the formation of calcium carbonates implies uptake of carbonate ions, jointly balanced by a decrease of hydrogenocarbonate ions and thus by a proton generation. This value is thus proportional to the amount of produced calcium

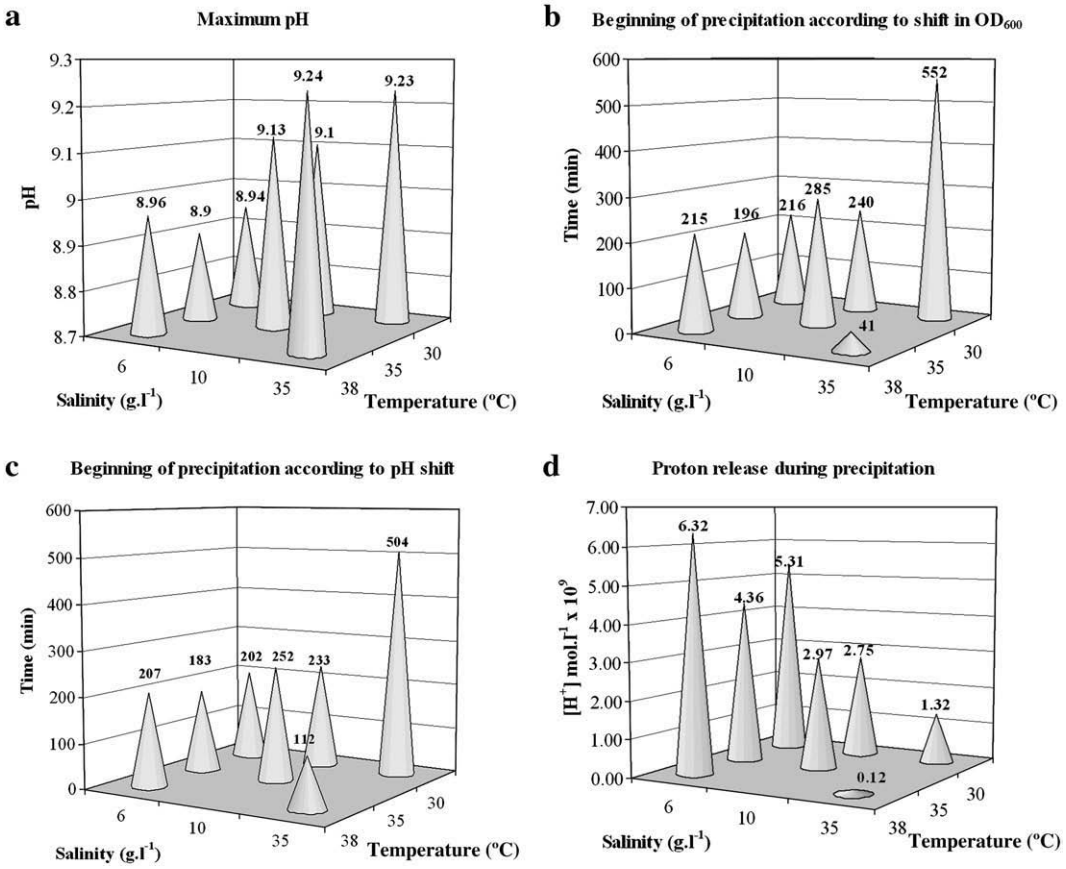

Fig. 5. Experiments conducted in BCC with different salinities (5.8, 13.5 and 35.0 $g.l^{-1}$) and temperatures (30, 35 and 38 °C). Solutions were in contact with closed air atmosphere (1 bar). For each experiment, maximum pH value reached (a; Average Standard Error (ASE) = 0.036), estimation of the beginning of the precipitation according to the shift of OD_{600} (b; ASE = 3.93) or pH (c; ASE = 2.60) and quantity of protons released during the precipitation (d; ASE = 0.36) are displayed.

Please cite this article as: Dupraz, S., et al., Experimental approach of CO_2 biomineralization in deep saline aquifers, Chem. Geol. (2009), doi:10.1016/j.chemgeo.2008.12.012

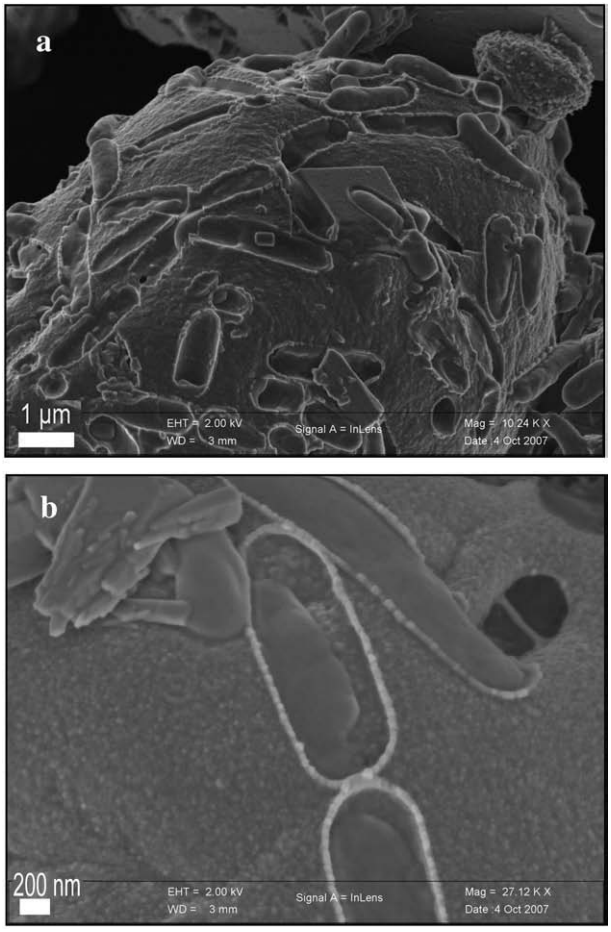

Fig. 6. SEM observations in secondary electron mode (SE) of precipitates recovered at the end of the BCC experiment running at 30 °C in (a) air with salinity of 13.5 $g.l^{-1}$ and (b) N_2 with salinity of 5.8 $g.l^{-1}$. Numerous *Bacillus pasteurii* cell prints are visible on the precipitate surfaces. The mineral matrix appears to be separated from the bacteria by a gap of about ten nanometers (a). Contacts between these cell prints lead to conclude that this specific biomineralization is linked to the cell walls (b). The matrix of the cell wall has been already recognized as a specific site of biomineralization (Castanier et al., 1999; Castanier et al., 2000; Lian et al., 2006). Nevertheless, its organic structure could be partially responsible for the crystal growth inhibition observed between the cell remaining and wall (Addadi et al., 2003; Rodriguez-Navarro et al., 2003).

carbonate if we do consider the contributions of ureolysis and gas diffusion as constant during the precipitation. These results show that stronger precipitations are observed at low salinities. Again, temperature effects are small. Solid-state samples resulting from these experiments were collected and observed by SEM. Fig. 6a and b display an example of those calcium carbonate precipitates containing visible bacterial prints.

3.4. Gas phases

A last set of BCC experiments, carried out under standard salinity and temperature conditions (i.e. S=5.8 $g.l^{-1}$ at 30 °C with agitation) was designed for investigating the effect of the atmosphere overlaying the experiment (Fig. 7). First, results of tests performed in a closed 1 bar atmosphere show no qualitative differences between air and N_2. To the contrary, the blank tests that were run under the same standard conditions but in contact with open atmosphere display very different pH maximum values compared to those in closed atmospheres (8.37 ± 0.05 against 8.91 ± 0.05 respectively, Fig. 7). Results obtained using pure CO_2 atmosphere are compiled in Figs. 7-9. Under 1 bar of CO_2, the pH rapidly shifts from 6.0 to a value of about 4.3, then slowly increases during about 55 h to a value of 8.0, as reported in Figs. 7 and 8. At this stage, some precipitation occurs simultaneously with a kink in pH evolution observed toward the end of the experiment as shown in Fig. 8. SEM observations of these precipitates indicate presence of dominant aragonite with splitting needle forms covered by numerous submicrometric spherules identified as bacterial spores on the basis of their morphology and high phosphorus and sulphur contents highlighted by EDS analysis (Fig. 9). Batch reactor tests with pressure of 5 bar in the same conditions display small alkalinization and no precipitation despite a good steadiness of the OD_{600} (+0.5 pH unit for a maximum pH of 4.87).

4. Discussion

4.1. Effect of calcium

A first important observation is that some calcium carbonate precipitation could be observed even in nominally calciumless experiments (Figs. 2d and 3). Despite the washing steps performed before inoculation, the cells could indeed still contain enough calcium from their initial culture medium (i.e. brain heart broth) thus generating, after cellular lysis, significant calcium carbonate precipitation. Furthermore, some authors have shown that biofilm polymers formed during bacterial growth may strongly bind calcium ions and that this fraction of calcium is then hardly removed by simple washing steps (e.g. Dupraz and Visscher, 2005; Braissant et al., 2007). Nevertheless, this precipitation remained weak, consistently with no detection of the pH decrease usually associated to carbonate precipitation (e.g. Fig. 2a). Additionally, the calcium carbonates collected from those calciumless experiments display different morphologies compared to those observed in calcium-bearing experiments and show numerous confluent cell prints in the solid (Fig. 3). This particular morphology is likely due to the more elevated cell/mineral ratio of these experiments. Another important observation is that the rate of alkalinization in AGW free of calcium, assessed from the amount of HCl added, is slower than in the case of the standard AGW (Fig. 2c and d). This positive effect of calcium on the rate of pH increase is consistent with previous observations which demonstrated that *Bacillus subtilis* growth was dependent on calcium availability (Herbaud et al., 1998). Finally, the test in AGW free of calcium shows an increase of the rate of alkalinization at about 8 h (Fig. 2d). As previously interpreted in Dupraz et al. (2009—this issue), this is linked to the outgassing of CO_2 occurring above a threshold of ureolysis. This effect is not detectable in standard tests conducted in the presence of calcium due to the rapid and strong calcium carbonate precipitation.

4.2. Biomineralization and bacterial survival

Before calcium carbonate precipitation, the turbidity of the medium remains quite constant. However, as highlighted in Fig. 4, the MPN of Mac

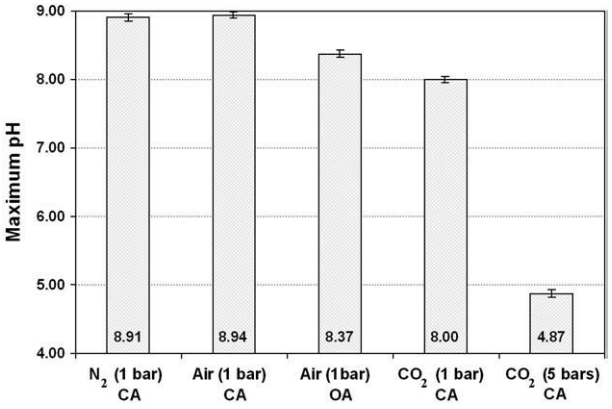

Fig. 7. Maximum pH values reached during experiments with various atmospheres. CA is referring to closed atmosphere (namely BCC and circulation cell experiments in standard conditions) and OA to open atmosphere (test in pH stat associated with the calcium experiments, see text).

Please cite this article as: Dupraz, S., et al., Experimental approach of CO_2 biomineralization in deep saline aquifers, Chem. Geol. (2009), doi:10.1016/j.chemgeo.2008.12.012

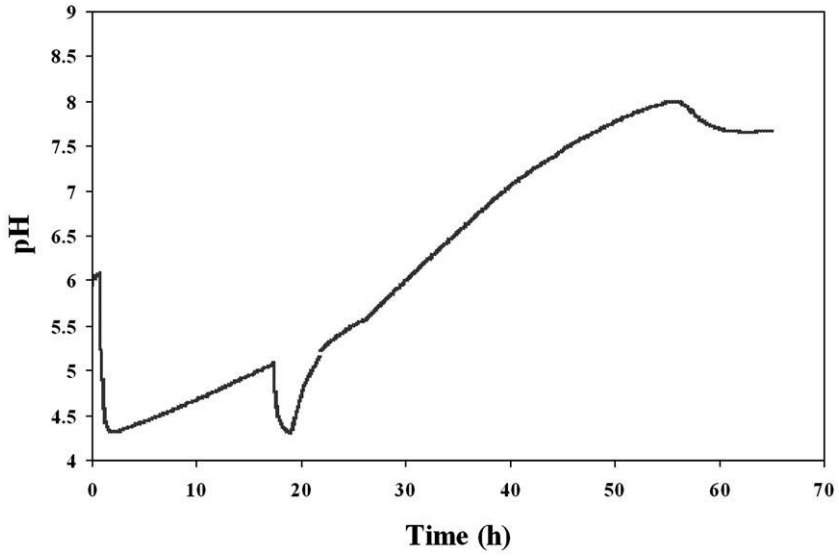

Fig. 8. pH evolution in AGW (5.8 g.l^{-1}) at 30 °C with a closed CO_2 atmosphere of 1 bar. Three decreases are observed; the first one (first hour) corresponds to the dissolution of CO_2 into the AGW, the second (after 18 h) is an artefact due to an accidental flush of CO_2 and the third (after 55 h) is due to calcium carbonate precipitation.

Grady is decreasing rapidly before the calcium carbonate precipitation stage, indicated by pH drop. Many cells detected by spectrophotometry and accounting for the OD_{600} are thus no longer alive. This supports the hypothesis of a cellular nucleation step initiating the biomineralization process, as discussed previously by McConnaughey and Whelan (1997), Hammes et al. (2003) and Dupraz et al. (2009—this issue). Likely favored by calcium accumulation, biomineralization begins with precipitation of amorphous calcium phosphates either in the cytoplasm or at cell surfaces leading to cell lysis (Dupraz et al., 2009—this issue). Subsequent calcium carbonate growth then occurs on phosphates serving as nucleation sites. This process explains that the OD_{600} slightly shifts before the main precipitation stage, as observed in Fig. 2b and c. It also explains that pH decrease usually occurs before OD_{600} decrease (Fig. 5b and c) since calcium phosphate cellular precipitation is releasing protons without changing cellular morphologies.

After the abrupt decreases in pH and OD_{600}, i.e. once most of calcium carbonates precipitation has occurred, the MPN of Mac Grady recovers, indicating that the number of viable *B. pasteurii* is increasing in the medium until it comes close to its initial level by the end of the experiments (Fig. 4). Since the AGW is not suited for sustaining the heterotrophic growth of *B. pasteurii* (this strain does not accept urea nor inorganic carbon as sources for carbon assimilation), the only source of carbon, phosphorus and other nutrients available is the one initially carried by the inoculum. Organic matter coming from cell lysis may have been thus used by the new generation of surviving cells and spores. Because the OD_{600} is continuously decreasing over the whole experiment (Fig. 4), this phenomenon cannot be attributed to the recovery of free-living cells in the solution. A possible explanation is the formation by new recovering cells of spores or biofilms attached to the newly formed precipitates, and thus not contributing to the turbidity.. Both bacterial aggregates and spores were indeed systematically observed in these samples.

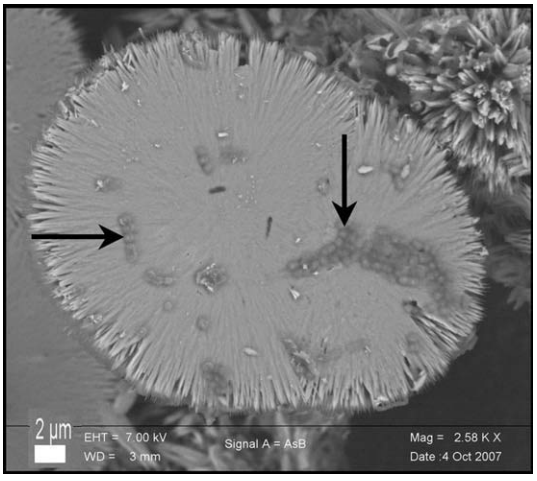

Fig. 9. SEM BSE image of precipitates yielded by the CO_2 atmosphere experiment (1 bar) shown in Fig. 8. The precipitates show a high density of submicrometric spores (indicated by arrowheads) laying on typical dumbbell-shaped aragonite spherulites.

4.3. Effect of temperature and salinity

Considering that CO_2 saturation level of the solution is decreased by higher temperatures and salinities, raising these two parameters will enhance the degassing and thus act in favor of faster rates of pH increase (Stumm and Morgan, 1996). Theoretically, the metabolic activity of *B. pasteurii* is known to fit the studied ranges of temperature and salinity (respectively, 30–38 °C and 5.8–35.0 g.l^{-1}): the strain can sustain salinities up to values as high as 58 g.l^{-1} (Kuhlmann and Bremer, 2002) and its optimal growth temperature was experimentally determined around 38 °C (Appendix A). Regarding enzymatic activity, maximal tested temperatures are far from denaturation temperatures of ureases (70 °C, see Illeová et al., 2003) and high salinity values are known to stabilize urease solubility and quaternary structure (Bhowmick and Jagannadham, 2006). The absence of evidence for a temperature effect in the present study can be explained by the fact that ureolysis is kinetically limited by another factor, likely the transport and diffusion of urea inside the cell, as already proposed by Magaña-Plaza and Ruiz-Herrera (1967). Although it was generally admitted that urea could freely diffuse through phospholipidic membrane, several authors have demonstrated that active transport is implicated in the increase of cytoplasm urea concentration (Mobley and Hausinger, 1989; Beckers et al., 2004; Radke et al., 2005). If the ureolytic system is endoplasmic, it also means that salinity would not directly affect the urease activity.

Larger salinities positively affect alkalinization rates but also increase the time delay before calcium carbonate precipitation begins (Fig. 5b and c). This is rather counterintuitive and different from predictions of simple models (Dupraz et al., 2009—this issue). Furthermore, in abiotic systems, increasing the ionic strength is recognized to accelerate kinetics of calcite growth (e.g. Zhang and Dawe, 1998). Since salinity is mostly adjusted by changing NaCl concentrations, this behavior might reveal specific effects

Please cite this article as: Dupraz, S., et al., Experimental approach of CO_2 biomineralization in deep saline aquifers, Chem. Geol. (2009), doi:10.1016/j.chemgeo.2008.12.012

associated to sodium ions (Hammes et al., 2003; Padan et al., 2005), which could accelerate ureolysis but at the same time decrease the concentration of calcium in the medium by inducing more efficient Ca uptake within cells. Indeed, in *Bacillus* species, Na^+ is mainly used in replacement of the proton gradient, which is unlikely to be sustainable in the alkaline AGW. Assimilation of nutrients as well as flagellum rotation are thus supposed to be maintained by Na^+ gradients (Yumoto, 2002). This mechanism has been demonstrated for glutamine uptake in *B. pasteurii* (Jahns, 1994). Calcium and urea could thus be possibly assimilated by antiporters or symporters using this gradient, and in accordance be directly influenced by the sodium concentration of the medium. An increase in salinity by addition of NaCl salt would thus favor ureolysis by allowing a more efficient transport of urea but also would reduce the level of saturation in the bulk aqueous phase by increased up taking of calcium ions. This could explain the apparent contradiction between the tendencies observed in Fig. 5a, b and c. Under strong salinities, however, the bacteria would become more vulnerable to an internal precipitation and, to some extent, their ability to accommodate these ions in their cytoplasm by the use of binding proteins (Herbaud et al., 1998) might be overwhelmed. The case of the test at 38 °C and S = 35 $g.l^{-1}$ can be interpreted that way: although it is the one that shows the strongest initial alkalinization (Fig. 5a), it is also the first to display a small precipitation (Fig. 5d) that precedes the pH fall (Fig. 5b and c). This delay of precipitation could also be explained by the presence of exopolymers often secreted by stressed bacteria affected in the present case by the salinity increase. In that case, a biofilm would trap calcium ions, as described previously.

4.4. Effect of the gas composition

An important result is that, even under 1 bar of CO_2, *B. pasteurii* is able to induce alkalinization of the AGW and subsequent calcium carbonate precipitation (Figs. 7 and 8). *B. pasteurii* has therefore demonstrated its ability to sustain ureolysis in an initial acidic medium. Nevertheless, an experiment conducted with 5 bar of CO_2 partial pressure yielded no calcium carbonate production and only marginal alkalinization (Fig. 7). Beyond the inactivation of bacteria due to high CO_2 partial pressure (see below) and to low pH, this could likely be linked to the buffering power of the dissolved inorganic carbon system which may prevent ureolysis to raise the pH. Indeed, increasing CO_2 partial pressures from 1 bar to more than 5 bar will not change pH by much (e.g. see Toews et al., 1995). On the opposite, the amount of dissolved inorganic carbon present in solution is increasing proportionally with CO_2 partial pressure. Consequently, under higher CO_2 partial pressures, bacteria will have to achieve more ureolysis to overcome acidic conditions and they will be exposed for a longer period to an acidic environment.

Both tested conditions (i.e. 1 and 5 bar) are still far from the conditions potentially encountered in CO_2 geological storage sites where much higher partial pressures of CO_2 are expected. Moreover, supercritical CO_2 fluids are also acknowledged to be strong organic and dehydrating solvents that have been often used to wash and sterilize chirurgical tools (Wu et al., 2006). In consequence, to overcome the CO_2 acidic buffering and toxicity, future investigations should focus on acidotolerant strains in peripheral zones were CO_2 partial pressure is reduced and thus compatible with biomineralization processes. Alkalinizing bacteria such as *B. pasteurii* could still have a positive impact on CO_2 mineralization into solid carbonates quite far away from the injection point, where pH has reached values above 4.5–5. Note that in the case of injection in basic or ultrabasic rocks, stabilization to pH 4–5 may be achieved rapidly (e.g. Daval et al., 2009—this issue), close to the injection point.

5. Conclusion

In this work, we described an experimental approach allowing investigation of the potential of the ureolytic strain, *B. pasteurii*, for CO_2 transformation into solid carbonate phases under environmental conditions (i.e. temperatures and salinities) of saline aquifers equilibrated with up to 5 bar CO_2 partial pressure and relevant to CO_2 geological sequestration. Increasing salinities (5.8, 13.5 and 35.0 $g.l^{-1}$) and specific concentrations of calcium ions are shown to have a positive effect on the rate of pH increase in the investigated solutions, whereas the effect of increasing temperatures (30, 35 and 38 °C) is less important. The mechanism by which salinities positively affect ureolysis rates is likely related to the effect of sodium ions on exchanges of urea and calcium between cells and medium. The observed decorrelation between ureolysis efficiency and calcium carbonate precipitation rates is better explained by cellular calcium uptake, favored in high salinity media. Precipitation of calcium carbonate is shown to be a deleterious event for cells. The bacterial population can however somewhat recover by heterotrophic growth using organic carbon and nutrients liberated in the medium once precipitation is over. Finally, *B. pasteurii* is shown to be able to induce pH increase and subsequent calcium carbonate precipitation in an AGW equilibrated with 1 bar of CO_2. This suggests that acidification induced by CO_2 injection in the subsurface can be counterbalanced by alkalinizing bacterial activity as far as the microorganisms can overcome the buffering power of the dissolved inorganic carbon. A large variety of aerobic and anaerobic microorganisms displays potentials for pH increase similar to that of *B. pasteurii*, and could thus be responsible for the initiation or development of CO_2 transformation into solid carbonates. Subsurface environments are by a majority without oxygen but CO_2 injection may induce medium oxygenation and aerobic stress for endogenic microbial communities. As a consequence, both anaerobic and aerobic metabolisms have to be considered. Of particular interest are the sulfate reducing bacteria, likely abundant in the subsurface, which consume protons while reducing sulphate into sulphide. In that perspective, microbial mediated processes favoring carbonate precipitation do not have to be eluded as far as they could strongly enhance the stability of the CO_2 containment by cementing the borders or even immobilizing significant amounts of injected CO_2 into solid carbonates.

Acknowledgements

We wish to warmly thank Michel Magot and Alain Bonneville for their contributions and advices. This work was supported by the Centre de Recherches de Stockage Géologique du CO_2. (IPGP/TOTAL/SCHLUMBERGER) and the GéoCarbone-Carbonatation project funded by the French ANR in 2005 (ANR-05-C02-009-01). This is IPGP contribution No. 2391.

Appendix A

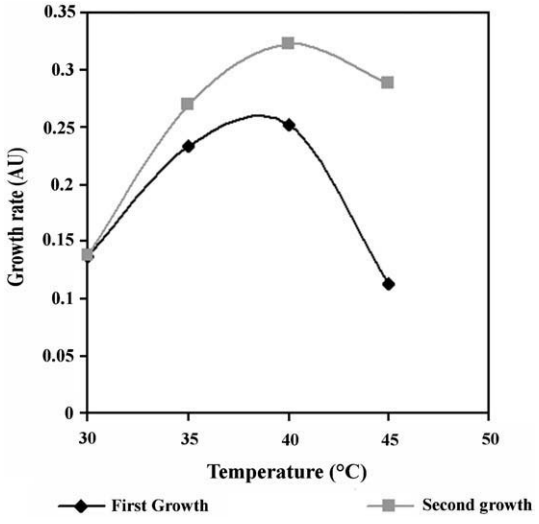

Fig. A1 *B. pasteurii* growth rate in brain heart broth medium complemented with 2% urea highlighting optimal values around 38 °C.

Please cite this article as: Dupraz, S., et al., Experimental approach of CO_2 biomineralization in deep saline aquifers, Chem. Geol. (2009), doi:10.1016/j.chemgeo.2008.12.012

First growth measurements were carried out during the exponential phase after the first inoculation. Second were accomplished by inoculating the medium with fresh material of the first growth series.

References

Addadi, L., Raz, S., Weiner, S., 2003. Taking advantage of disorder: amorphous calcium carbonate and its roles in biomineralization. Adv. Mater. 15 (12), 959–970.

Amend, J.P., Teske, A., 2005. Expanding frontiers in deep subsurface microbiology. Paleogeogr. Paleoclimatol. Paleoecol. 219 (1–2), 131–155.

Azaroual, M., Fouillac, C., Matray, J.M., 1997. Solubility of silica polymorphs in electrolyte solutions, II. Activity of aqueous silica and solid silica polymorphs. Chem. Geol. 140 (3), 167–179.

Beckers, G., Bendt, A.K., Krämer, R., Burkovski, A., 2004. Molecular identification of the urea uptake system and transcriptional analysis of urea transporter- and urease-encoding genes in *Corynebacterium glutamicum*. J. Bacteriol. 186 (22), 7645–7652.

Bhowmick, R., Jagannadham, M., 2006. Multiple intermediate conformations of jack bean urease at low pH: anion-induced refolding. Protein J. 25 (6), 399–410.

Braissant, O., Decho, A.W., Dupraz, C., Glunk, C., Przekop, K.M., Visscher, P.T., 2007. Exopolymeric substances of sulfate-reducing bacteria: interactions with calcium at alkaline pH and implication for formation of carbonate minerals. Geobiol. 5 (4), 401–411.

Castanier, S., Le Métayer-Levrel, G., Perthuisot, J.-P., 1999. Ca-carbonates precipitation and limestone genesis: the microbiogeologist point of view. Sediment. Geol. 126 (1), 9–23.

Castanier, S., Le Metayer-Levrel, G., Perthuisot, J.-P., 2000. Bacterial roles in the precipitation of carbonates minerals. In: Riding, R.E., Awramik, S.M. (Eds.), Microbial Sediments. Springer-Verlag, Berlin, pp. 32–39.

Daval, D., Martinez, I., Corvisier, J., Findling, N., Goffé, B., Guyot, F., 2009. Carbonation of Ca-bearing silicates, the case of wollastonite: experimental investigations and kinetic modeling. Chem. Geol. (this issue).

Dupraz, C., Visscher, P.T., 2005. Microbial lithification in marine stromatolites and hypersaline mats. Trends Microbiol. 13 (9), 429–438.

Dupraz, S., Parmentier, M., Ménez, B., Guyot, F., 2009. Experimental study and modeling of calcium carbonate precipitation induced by *Bacillus pasteurii*. Chem. Geol. (this issue).

Ferris, F.G., Stehmeier, L.G., Kantzas, A., Mourits, F.M., 1996. Bacteriogenic mineral plugging. J. Can. Petrol. Technol. 35, 56–61.

Ferris, F.G., Phoenix, V., Fujita, Y., Smith, R.W., 2003. Kinetics of calcite precipitation induced by ureolytic bacteria at 10 to 20 °C in artificial groundwater. Geochim. Cosmochim. Acta 67 (8), 1701–1722.

Hammes, F., Boon, N., de Villiers, J., Verstraete, W., Siciliano, S.D., 2003. Strain-specific ureolytic microbial calcium carbonate precipitation. Appl. Environ. Microbiol. 69 (8), 4901–4909.

Harder Nielsen, T., Bonde, T.A., Sörensen, J., 1998. Significance of microbial urea turnover in N cycling of three Danish agricultural soils. FEMS Microbiol. Ecol. 25 (2), 147–157.

Haszeldine, R.S., Quinn, O., England, G., Wilkinson, M., Shipton, Z.K., Evans, J.P., Heath, J., Crossey, L., Ballentine, C.J., Graham, C.M., 2005. Natural geochemical analogues for carbon dioxide storage in deep geological porous reservoirs, a United Kingdom perspective. Oil Gas Sci. Technol. 60, 33–49.

Herbaud, M.L., Guiseppi, A., Denizot, F., Haiech, J., Kilhoffer, M.C., 1998. Calcium signalling in *Bacillus subtilis*. Biochim. Biophys. Acta 1448 (2), 212–226.

Hugues, B., Plantat, J.L., 1983. Calcul des limites d'acceptation du nombre le plus probable dans le cas ou le nombre d'inoculums par dilution est important. Chemosphere 12 (11), 1679–1684.

Illeová, V., Polakovic, M., Stefuca, V., Acai, P., Juma, M., 2003. Experimental modelling of thermal inactivation of urease. J. Biotechnol. 105 (3), 235–243.

Intergovernmental Panel on Climate Change (IPCC), 2007. Climate Change 2007: Synthesis Report. Cambridge University Press, New-York. (submitted, available for downloading at http://www.ipcc.ch, 52 pp).

Jahns, T., 1994. Ammonium-stimulated, sodium-dependent uptake of glutamine in *Bacillus pasteurii*. Arch. Microbiol. 161, 207–214.

Jahns, T., 1996. Ammonium/urea-dependent generation of a proton electrochemical potential and synthesis of ATP in *Bacillus pasteurii*. J. Bacteriol. 178 (2), 403–409.

Kuhlmann, A.U., Bremer, E., 2002. Osmotically regulated synthesis of the compatible solute ectoine in *Bacillus pasteurii* and related *Bacillus* spp. Appl. Environ. Microbiol. 68 (2), 772–783.

Lian, B., Hu, Q., Chen, J., Ji, J., Teng, H.H., 2006. Carbonate biomineralization induced by soil bacterium *Bacillus megaterium*. Geochim. Cosmochim. Acta 70 (22), 5522–5535.

Magaña-Plaza, I., Ruiz-Herrera, J., 1967. Mechanisms of regulation of urease biosynthesis in *Proteus rettgeri*. J. Bacteriol. 93 (4), 1294–1301.

McConnaughey, T.A., Whelan, J.F., 1997. Calcification generates protons for nutrient and bicarbonate uptake. Earth Sci. Rev. 42 (1), 95–117.

Ménez, B., et al., 2007. Impact of the deep biosphere on CO_2 storage performance. Geotechnologien Sci. Rep. 9, 150–163.

Mitchell, A.C., Ferris, F.G., 2005. The coprecipitation of Sr into calcite precipitates induced by bacterial ureolysis in artificial groundwater: temperature and kinetic dependence. Geochim. Cosmochim. Acta 69 (17), 4199–4210.

Mobley, H.L., Hausinger, R.P., 1989. Microbial ureases: significance, regulation, and molecular characterization. Microbiol. Rev. 53, 85–108.

Padan, E., Bibi, E., Ito, M., Krulwich, T.A., 2005. Alkaline pH homeostasis in bacteria: new insights. BBA–Biomembranes 1717 (2), 67–88.

Pedersen, K., 2000. Exploration of deep intraterrestrial microbial life: current perspectives. FEMS Microbiol. Lett. 185, 9–16.

Pokrovsky, O.S., Golubev, S.V., Schott, J., 2005. Dissolution kinetics of calcite, dolomite and magnesite at 25 °C and 0 to 50 atm pCO_2. Chem. Geol. 217, 239–255.

Radke, J., et al., 2005. Correlation between hydrogen isotope ratios of lipid biomarkers and sediment maturity. Geochim. Cosmochim. Acta 69 (23), 5517–5530.

Rodriguez-Navarro, C., Rodriguez-Gallego, M., Ben Chekroun, K., Gonzalez-Munoz, M.T., 2003. Conservation of ornamental stone by *Myxococcus xanthus*-induced carbonate biomineralization. Appl. Environ. Microbiol. 69 (4), 2182–2193.

Smith, D.G., Russell, W.C., Ingledew, W.J., Thirkell, D., 1993. Hydrolysis of urea by *Ureaplasma urealyticum* generates a transmembrane potential with resultant ATP synthesis. J. Bacteriol. 175 (11), 3253–3258.

Stocks-Fischer, S., Galinat, J.K., Bang, S.S., 1999. Microbiological precipitation of $CaCO_3$. Soil Biol. Biochem. 31, 1563–1571.

Stumm, W., Morgan, J.J., 1996. Aquatic Chemistry, Chemical Equilibria and Rates in Natural Waters, 3rd edition. John Wiley & Sons, New-York, 1022 p.

Swensen, B., Bakken, L.R., 1998. Nitrification potential and urease activity in mineral subsoil. Soil Biol. Biochem. 30 (10/11), 1333–1341.

Toews, K.L., Shroll, R.M., Wai, C.M., Smart, N.G., 1995. pH-defining equilibrium between water and supercritical CO_2. Influence on SFE of organics and metal chelates. Anal. Chem. 67, 4040–4043.

Wu, S.-M., et al., 2006. Quantum-dot-labeled DNA probes for Fluorescence In Situ Hybridization (FISH) in the microorganism *Escherichia coli*. ChemPhysChem 7, 1062–1067.

Yoon, J.H., Lee, K.C., Weiss, N., Kho, Y.H., Kang, K.H., Park, Y.H., 2001. *Sporosarcina aquimarina* sp. nov., a bacterium isolated from seawater in Korea, and transfer of *Bacillus globisporus* (Larkin and Stokes 1967), *Bacillus psychrophilus* (Nakamura 1984) and *Bacillus pasteurii* (Chester 1898) to the genus *Sporosarcina* as *Sporosarcina globispora* comb. nov., *Sporosarcina psychrophila* comb. nov. and *Sporosarcina pasteurii* comb. nov., and emended description of the genus *Sporosarcina*. Int. J. Syst. Evol. Microbiol. 51, 1079–1086.

Yumoto, I., 2002. Bioenergetics of alkaliphilic *Bacillus* sp. J. Biosci. Bioeng. 93 (4), 342–353.

Zhang, Y., Dawe, R., 1998. The kinetics of calcite precipitation from a high salinity water. Appl. Geochem. 13, 177–184.

Please cite this article as: Dupraz, S., et al., Experimental approach of CO_2 biomineralization in deep saline aquifers, Chem. Geol. (2009), doi:10.1016/j.chemgeo.2008.12.012